Published in final edited form as:
Ultrasonics. 2009 March ; 49(3): 389–394. doi:10.1016/j.ultras.2008.10.011.

Vibro-acoustography Imaging of Permanent Prostate Brachytherapy seeds in an excised human prostate — Preliminary Results and Technical Feasibility

F.G. Mitri[*,1], **B.J. Davis**[2], **M.W. Urban**[1], **A. Alizad**[1], **J.F. Greenleaf**[1], **G.H. Lischer**[3], **T.M. Wilson**[3], and **M. Fatemi**[1]

[1]Mayo Clinic, Department of Physiology and Biomedical Engineering, Ultrasound Research Laboratory, 200 First Street SW, Rochester, MN 55905

[2]Mayo Clinic, Department of Radiation Oncology, 200 First Street SW, Rochester, MN 55905

[3]Mayo Clinic, Department of Urology, 200 First Street SW, Rochester, MN 55905

Abstract

Objective—The objective in this work is to investigate the feasibility of using a new imaging tool called vibro-acoustography (VA) as a means of permanent prostate brachytherapy (PPB) seed localization to facilitate post-implant dosimetry (PID).

Methods and Materials—Twelve OncoSeed (standard) and eleven EchoSeed (echogenic) dummy seeds were implanted in a human cadaver prostate. Seventeen seeds remained after radical retropubic prostatectomy. VA imaging was conducted on the prostate that was cast in a gel phantom and placed in a tank of degassed water. 2-D magnitude and phase VA image slices were obtained at different depths within the prostate showing location and orientation of the seeds.

Results—VA demonstrates that twelve of seventeen (71%) seeds implanted were visible in the VA image, and the remainder were obscured by intra-prostatic calcifications. Moreover, it is shown here that VA is capable of imaging and locating PPB seeds within the prostate independent of seed orientation, and the resulting images are speckle free.

Conclusion—The results presented in this research show that VA allows seed detection within a human prostate regardless of their orientation, as well as imaging intraprostatic calcifications.

Keywords

Brachytherapy; Prostate cancer; Seed; Ultrasound; Vibro-acoustography; 43.20.+g General linear acoustics; 43.25.+y Nonlinear acoustics; 43.40.+s Structural acoustics and vibration; 43.35.+d Ultrasonics, quantum acoustics, and physical effects of sound

*Corresponding Author: F.G. Mitri Mayo Clinic College of Medicine 200 First St SW Rochester, MN 55905 Email: E-mail: mitri.farid@mayo.edu , E-mail: mitri@ieee.org.

1. Introduction

Prostate cancer is the most common cancer in males in the United States. When prostate cancer is suspected, a transrectal ultrasound-guided prostate biopsy is performed to establish the diagnosis [1]. If the biopsy confirms the presence of cancer, treatment may occur shortly thereafter, or a watchful waiting approach may be undertaken. Radical prostatectomy, external beam radiation therapy (EBRT) and brachytherapy are widely used as definitive therapies for localized cancer.

Brachytherapy (BT) [2-4] is one method that may be used to deliver high radiation doses to the prostate, while sparing normal tissues that are located adjacent to the prostate. In BT, transrectal ultra-sonography (TRUS) is used to guide the placement of encapsulated 125Iodine (125I) or 103 Palladium (103Pd) seeds throughout the prostate gland [5]. Typical seeds are cylindrical in shape having a diameter of 800 microns and length of 4.5 mm. One possible drawback of PPB implantation is the potential for under-dosing a portion or portions of the gland. This may occur if seeds are misplaced during the procedure.

Dynamic real-time calculation of the dose distribution based on actual seed placement during the implantation procedure is recommended to optimize the treatment planning procedure [6-10]. Magnetic resonance imaging (MRI) provides improved visualization of the prostate and its surrounding anatomy [11], which should make it the image modality of choice to guide brachytherapy seed placement. However, the principal limitation to its routine use in PPB, is the complex and challenging environment inherent to MRI technology and the constrained ergonomics of closed-bore scanners. Computed tomography (CT) has been very useful in identifying seeds and is the standard for determining postimplantation dosimetry. However, with CT, the delineation of the prostate gland and the adjacent structures is limited because of relatively weak intrinsic contrast among soft tissues. Furthermore, because the prostate (pseudo)capsule is not visualized on CT, assessment of the volume of the gland is difficult and inaccurate [12,13]. Transperineal, three-dimensional (3-D) transperineal— and transrectal-guided ultrasonography were developed as other alternatives [5,14]. Ultrasound techniques predicted prostate size with a high degree of accuracy but seeds give rise to artifacts [15], and movement of the gland during imaging may hamper evaluation of the prostate and seed distribution.. Although a tissue/titanium interface is expected to give excellent ultrasound echoes, practical experience indicates that a majority of implanted seeds are difficult to detect with ultrasound imaging. Typically, only 30%-50 % of the encapsulated seeds are identified under *in vivo* conditions by scanning the whole prostate volume [16,17]. Thus, TRUS examination of the prostate is of limited value for post-implant seed localization.

Recent breakthroughs in imaging have catalyzed the development of novel techniques, such as “elasticity imaging methods” that are sensitive to the elastic properties of tissue [18-20]. Acoustical radiation force-based methods are successfully used in many biomedical applications including ophthalmology [21], detecting and characterizing lesions [22], staging deep venous thrombosis [23], imaging breast calcifications [24], etc. One possible method among these techniques that can be used to improve seed visualization and enhance the potential for real-time quantitative and meaningful feedback during the procedure is Vibro-acoustography (VA) [25]. Previous work with VA has shown substantial capabilities of this technique versus pulse-echo ultrasound to detect PPB seeds at various orientations in an idealized laboratory setting, in which no human tissue was involved [26]. Moreover, quantitative analysis has confirmed the validity of this approach [27], yet evaluation of the seed localization in a biological prostate has not been previously undertaken.

The purpose of the present study is to examine PPB seed imaging in an excised human prostate using the VA technique. This is an interim step to the realistic case of a prostate in a patient.

The objective of this research is to show the feasibility of VA in imaging PPB seeds in an excised human prostate. Here, a fresh cadaver prostate is implanted with standard and echogenic seeds. Then, images showing seed location and orientation in the excised prostate are produced. The results as well as the potential use of VA in detecting PPB seeds are discussed, and a summary is presented.

2. Materials and methods

The VA imaging system that is used to scan the prostate is described in Fig. 1. The VA imaging technique produces a map of the mechanical response of an object to a dynamic force applied at each point. The method utilizes ultrasound radiation force to remotely exert a localized oscillating stress field, or in other words a tapping force, at a desired frequency within, or on the surface of an object, and records the resultant acoustic response or acoustic emission. This acoustic response, which is normally in the low kHz range, is a function of the viscoelastic properties of the object and can be used to produce an image of the object. To confine the oscillating radiation stress to the desired region, VA uses two ultrasound beams driven at slightly different frequencies, propagating along separate paths. The beams are arranged to cross each other at their respective foci, and thus produce a modulated field at a confined, small cross-sectional region. The mix of two ultrasound beams operating at different frequencies and intersecting in space generates a radiation force on the object by which multiple other frequencies are produced, including a component at the difference of the two operating frequencies. The object to be imaged is placed at the joint focal plane of the ultrasound transducer, also known as the scanning plane. Depending on the elastic properties of the object, the radiation force may cause a portion of the object, or the entire object, to vibrate at the difference frequency. The acoustic emission resulting from object vibration is received by a hydrophone which is placed nearby. If the wavelength of vibration is large compared with the object size, the acoustic emission pressure field is almost omnidirectional. Therefore, at low frequencies, the hydrophone position is not a critical parameter in the measurement of the acoustic emission signal. To form an image, the focal point of the transducer is moved across the scanning plane on the object in a raster pattern. The acoustic emission is received at each position, and an image is formed by displaying the magnitude (or phase) of such signals at corresponding positions on the image plane. The spatial resolution of this imaging method is determined by the ultrasound beam-width at the focal plane, which is normally of the order of the incident ultrasound wavelength.

For this experiment, the two ultrasound beams were generated by a two-element homemade confocal transducer with a diameter of 45 mm, a focal distance of 70 mm and a center frequency of 3 MHz. The elements were driven by two continuous-wave (CW) signals at frequencies of 3 MHz and 3 MHz + 20 kHz. The driving radio frequency (RF) signals were obtained from two stable function generators (HP 33120 A, Hewlett-Packard Company, Houston TX, USA). The transducer was mounted on a three-axes positioning system and immersed in a tank of degassed water to ensure good acoustical coupling. For this particular confocal transducer, the on-and off-axes resolutions, defined as the focal spot at full-width at half-maximum, were 10 and 0.7 mm respectively. The acoustic emission pressure field was detected by a submerged audio hydrophone (Model ITC—6050 C, Santa Barbara CA, USA) with sensitivity —157dB re 1V/μPa, diameter and length of 50 and 200 mm respectively (sensitive area of 70 mm), and frequency response between 1 Hz and 60 kHz, placed in the water tank. The signal received was bandpass filtered and amplified (Stanford Research Systems, SR650, Sunnyvale CA, USA) to eliminate noise, then digitized by a 12-bits/sample digitizer (National Instruments VXI-1000, Austin TX, USA) at a rate sufficiently higher than the Nyquist rate. The data were then recorded on a computer. Magnitude and phase images were produced after processing the data. The phase images acquired in the experiment contained phase wraps. Therefore, the measured phase should be processed (unwrapped) prior to use as a comprehensible data. To

provide a continuous phase image, two-dimensional phase unwrapping was performed. An unweighted least-squares multigrid phase unwrapping algorithm was used [28]. This method is iterative and operates on multiple scales to eliminate high-frequency components of the error. Absence of noise in the images presented leads us to believe that no errors were encountered. The phase unwrapping process performs very quickly with C code provided in Ref. [28] implemented on a modern computer.

A cadaver prostate was implanted with the patient in the dorsal lithotomy position using standard TRUS and fluoroscopic guidance within 24 hours of the patient's expiration. The seeds were implanted in the cadaver to simulate an actual PPB therapy procedure. Seed orientation and placement would have been different if the implantation procedure is performed within the excised prostate tissue. A total of 23 seeds, 12 standard and 11 echogenic, were implanted. Then, the prostate was removed via conventional radical retropubic prostatectomy (RRP) as performed by a urologic surgeon (G.H. Lischer). The cadaver prostate was then cast in formalin-catalyzed porcine gelatin (Sigma-Aldrich G2500 Type A, 300 bloom, Saint Louis MO, USA) at 15% concentration by volume to hold it in place. The gland was centered in the gelatin block having the dimensions $13\times13\times5$ cm^3. Seventeen seeds remained in the prostate following prostatectomy as determined by fluoroscopic imaging (Fig. 2). Six seeds were inadvertently extruded from the prostate during the extirpation even though they were implanted well within the gland. In addition, it was observed that the seeds were rearranged within the gland with the substantial prostate manipulation required during the RRP and placement in the gelatin block. All procedures used on the cadaver were approved by the Mayo Clinic Institutional Review Board (protocol ID 06-003629). The post-implanted prostate was then immersed in a tank of degassed water for scanning (Fig. 1).

Magnitude and phase VA images at different depths were acquired by scanning the transducer over the gland surface by a 1 mm incremental step for a total range of 24 mm deep inside the prostate gland. The images covered an area of 50 mm by 50 mm, scanned at 0.25 mm/pixel incremental step. Only representative magnitude and phase VA images taken at 1, 5, 10, and 15 mm deep from the surface of the prostate, showing seed location and orientation in the prostate are presented in Fig. 3 and 4, respectively. These VA images show some of the seeds at various angles. Other seeds were visible when the scan was performed at different depths. As the scan was performed in depth to cover the entire volume of the prostate, some of the seeds start to disappear from the VA image as they fall out of the focal region of the confocal transducer (See Figs. 3-(d), 4-(d)). After analyzing qualitatively the whole set of magnitude and phase VA images, 12 seeds were detected out of 17 (71%) seeds implanted within the prostate. The detection of seeds and images review were carried out by visual inspection as performed by urologists (GHL, TMW) and radiation oncologist (BJD). This preliminary result (detection rate of 71%) has already surpassed the seed detection rate typically reported for conventional TRUS in *in vivo* applications, to be approximately 30%-50% [16]. This detection rate should not be understood as an absolute value since one case (obtained from an *in vitro* study) is reported here.

3. Discussion

We have performed an initial study of imaging permanent prostate brachytherapy (PPB) seeds by vibroacoustography (VA). VA imaging of PPB seeds offers a unique advantage compared to pulse echo ultrasound because it is relatively insensitive to seed orientation. In addition, VA imaging enables detection of intra-prostatic calcifications as confirmed by histology. Calcifications are a common finding in the prostate and appear to be mostly associated with benign hyperplasia [29]. However, a recent report showed that calcifications can also occur in direct association with prostatic adenocarcinoma [29], although the incidence of this association is not as high as in breast carcinoma [30]. The results of this work are consistent

with those previously obtained in well-controlled laboratory experiments [26,27], and provide encouraging data for further evaluation of VA as a means of developing intraoperative-based dosimetry of PPB. Upon visual inspection of the magnitude and phase VA images (obtained at 20 kHz), it is noticeable that seeds are clearly identified and calcifications are evidently displayed. Such images have high spatial resolution, without speckle, good contrast, and high signal to noise ratio. For this specific excised prostate, the 71% seed detection rate within the prostate has provided an impetus to further develop, evaluate the performance, and optimize VA to achieve an improved seed detection rate and to evaluate this approach *in vivo*. The 29%-lack of seed detection was attributed to intra-prostatic calcifications near the center of the prostate gland (See Figs. 3 and 4) which reflect ultrasound waves and obscure the seeds. The choice of vibration frequency used in this experiment, 20 kHz, was determined based on experience with imaging breast calcifications. The selected difference frequency does not correspond to the resonance frequency of the seeds. The reason is that the seeds' first natural resonance frequency was estimated (using finite element analysis) to be around 150 kHz, a frequency that is beyond the sensitivity of our hydrophone. Further evaluation of other optimized vibration frequencies is warranted.

One also notices a contrast reversal in the magnitude images. This artifact may be the result of sound reverberations within the gel block. Moreover, interference of sound waves bouncing from the walls of the water tank may also contribute to the contrast change, depending on the waves' relative phases. This issue requires further investigation to properly study the effects of reverberations on the contrast of VA images.

The unwrapped phase of a vibration-based signal has been shown to provide unique high-contrast images [31]. The unwrapped phase of the acoustic emission from prostate tissue is relatively constant. The unwrapped phase contrast of the calcification differs with the focal distance. The borders of the calcification are well-defined in the unwrapped phase images. The brachytherapy seeds are well visualized for focal distances of 1-12 mm (Fig. 4-(a)-(d)). In the magnitude images (Fig. 3-(a)-(d)), the contrast of the seeds with respect to the surrounding tissue reverses with increasing focal distance; however, the seeds are always brighter than the surrounding tissue providing a positive contrast. This unwrapped-phase contrast mechanism may provide better visualization of embedded brachytherapy seeds for therapy monitoring.

The image spatial resolution improves as frequency increases. The transducer used in this experiment operated at 3.0 MHz which resulted of a lateral spatial resolution of 0.7 mm. VA image resolution would be better (< 0.7 mm) at ultrasound frequencies in the range of 5.0–7.5 MHz which is the range used in conventional transrectal ultrasound (TRUS) imaging [6].

In the present study, the scanning mechanism used for this experiment scans the object one point at a time, making the data collection a relatively lengthy process (up to 4 minutes per image covering an area of 50 mm by 50 mm). A long imaging time is not desirable for prostate imaging because body motions within this period can introduce "motion artifact" in the images and the procedure anesthesia time could be impractical. One way to reduce the scanning time significantly is to use electronic beam focusing and steering [32] providing high-speed scanning. Current work in our group is directed towards the development and testing of a linear array probe with dynamic focusing whereby the imaging time should be reduced by at least one order of magnitude.

Although VA uses ultrasound as a non-invasive energy source, the system properties are different from those of conventional pulse-echo ultrasound imaging (B-scan), and, in particular, TRUS. As a result, VA promises new diagnostic applications not normally offered by conventional ultrasound. A notable advantage of VA over pulse echo ultrasound is that VA can image PPB seeds practically at any angle [26], whereas TRUS imaging is highly sensitive

to seed orientation [33]. The seeds start to break up and each appears as two separate dots when they are imaged slightly off the perpendicular angle of incidence [33]. On the other hand, VA shows a considerable ability to detect the PPB seeds independent of their orientation. Therefore, VA is expected to detect randomly oriented seeds in and around the prostate, while TRUS can miss seeds depending on their angle relative to the beam axis. In addition to imaging soft tissue, VA can image stiff metallic implants, such as calcifications in breast [24,34] and carotid and iliac arteries [25] with great accuracy and efficiency. Furthermore, it has been shown that VA can detect very small hard objects, even breast microcalcifications [35] having diameters ranging from 0.1 to 1 mm.

The focus of the present study was to assess the capability of VA in detecting seeds in a human non pathologic prostate specimen. Cancerous prostatic tissue, as well as healthy prostatic tissue, may contain calcifications [29] of sizes comparable to PPB seeds. Once detected by the VA system, calcifications may therefore be confused with seeds, hence, producing false positives. It is doubtful, however, that the calcifications will be of the same three-dimensional size and shape of the seeds but this potential problem is nonetheless acknowledged. A similar problem also exists with conventional TRUS. In this initial *in vitro* study, no attempt has been made here to assess the false positive rate in seed detection. Further investigation is required to address this issue.

A key question raised for *in vivo* use of VA is whether the system can function properly at a reasonably low intensity level that is considered safe. Previous work [36] has shown that VA operates at intensities below the FDA recommended value [37] of 720 mW/cm^2. For this experiment, it was verified that using ultrasound intensities at or below the FDA recommended level was achieved. In comparison to fluoroscopy [38], where the use of X-Ray may be of modest concern for the safety of the operating room personnel and the patient, the operation of diagnostic level ultrasound used in VA is considered safe.

Another limitation is the result of two effects: phase aberration and sound speed variations in tissue. First, the ultrasound beams tend to defocus; second, the two beams fail to intersect at their mutual focal point. The first effect results in beam broadening, which in turn results in the loss of spatial resolution and decreased sensitivity due to decreased peak radiation intensity. The second effect results in similar outcomes. In addition, this effect may cause the beams to intersect at an unanticipated location in the object, and hence introduce image distortion.

4. Conclusion

These results represent the first study of the efficacy of using the VA technique for imaging PPB seeds in an excised human prostate *in vitro*. Results presented here show that VA allows detection regardless of seed orientation as well as imaging intraprostatic calcifications. These promising results suggest that VA may be useful as a clinical tool in seed localization for PPB. Ongoing work is directed towards evaluating the performance of VA in imaging PPB seeds in a large number of excised prostates. The design of specific probes for brachytherapy applications is currently under investigation.

Acknowledgements

Research supported by the National Institute of Health under Grant No. EB 00535-04, Grant No. CA 91956-06P2, and a Grant by Oncura Inc., Plymouth Meeting, PA. Disclosure: Parts of the techniques used here are patented by M. Fatemi and J.F. Greenleaf. The authors are grateful to M.A. Hadaway, W.N. Lajoie and R.R. Kinnick for technical and laboratory assistance.

REFERENCES

[1]. Brawer MK, Ploch NR, Bigler SA. Prostate-Cancer Tumor Location as Predicted by Digital Rectal Examination Transferred to Ultrasound and Ultrasound-Guided Prostate Needle-Biopsy. J. Cell. Biochem 1992:74–77. [PubMed: 1322917]

[2]. Beyer DC. The Evolving Role of Prostate Brachytherapy. Cancer Control 2001;8:163–170. [PubMed: 11326171]

[3]. Porter AT, Forman JD. Prostate Brachytherapy - an Overview. Cancer 1993;71:953–958. [PubMed: 8428345]

[4]. Syed AMN, Puthawala A, Sharma A, Gamie S, Londrc A, Cherlow JM, Damore SJ, Nazmy N, Sheikh KM, Ko SJ. High-Dose-Rate Brachytherapy in the Treatment of Carcinoma of the Prostate. Cancer Control 2001;8:511–521. [PubMed: 11807421]

[5]. Holm HH, Juul N, Pedersen JF, Hansen H, Stroyer I. Transperineal 125iodine seed implantation in prostatic cancer guided by transrectal ultrasonography. J. Urol 1983;130:283–286. [PubMed: 6876274]

[6]. Nag S, Beyer D, Friedland J, Grimm P, Nath R. American brachytherapy society (ABS) recommendations for transperineal permanent brachytherapy of prostate cancer. Int. J. Radiat. Oncol. Biol. Phys 1999;44:789–799. [PubMed: 10386635]

[7]. Blake CC, Elliot TL, Slomka PJ, Downey DB, Fenster A. Variability and accuracy of measurements of prostate brachytherapy seed position in vitro using three-dimensional ultrasound: An intra- and inter-observer study. Med. Phys 2000;27:2788–2795. [PubMed: 11190962]

[8]. Wei ZP, Gardi L, Downey DB, Fenster A. Automated localization of implanted seeds in 3D TRUS images used for prostate brachytherapy. Med. Phys 2006;33:2404–2417. [PubMed: 16898443]

[9]. Jain AK, Zhou Y, Mustufa T, Burdette EC, Chirikjian GS, Fichtinger G. Matching and reconstruction of brachytherapy seeds using the Hungarian algorithm (MARSHAL). Med. Phys 2005;32:3475–3492. [PubMed: 16372418]

[10]. Fichtinger G, Burdette EC, Tanacs A, Patriciu A, Mazilu D, Whitcomb LL, Stoianovici D. Robotically assisted prostate brachytherapy with transrectal ultrasound guidance - Phantom experiments. Brachytherapy 2006;5:14–26. [PubMed: 16563993]

[11]. Yu KK, Hricak H. Imaging prostate cancer. Radiologic Clinics of North America 2000;38:59–85. [PubMed: 10664667]

[12]. Roach M, FaillaceAkazawa P, Malfatti C, Holland J, Hricak H. Prostate volumes defined by magnetic resonance imaging and computerized tomographic scans for three-dimensional conformal radiotherapy. Int. J. Radiat. Oncol. Biol. Phys 1996;35:1011–1018. [PubMed: 8751410]

[13]. Rasch C, Barillot I, Remeijer P, Touw A, van Herk M, Lebesque JV. Definition of the prostate in CT and MRI: A multi-observer study. Int. J. Radiat. Oncol. Biol. Phys 1999;43:57–66. [PubMed: 9989514]

[14]. Stock RG, Stone NN, Wesson MF, Dewyngaert JK. A Modified Technique Allowing Interactive Ultrasound-Guided 3-Dimensional Transperineal Prostate Implantation. Int. J. Radiat. Oncol. Biol. Phys 1995;32:219–225. [PubMed: 7721619]

[15]. Nag S, Ciezki JP, Cormack R, Doggett S, DeWyngaert K, Edmundson GK, Stock RG, Stone NN, Yu Y, Zelefsky MJ. Intraoperative planning and evaluation of permanent prostate brachytherapy: Report of the American Brachytherapy Society. Int. J. Radiat. Oncol. Biol. Phys 2001;51:1422–1430. [PubMed: 11728703]

[16]. Su Y, Davis BJ, Herman MG, Robb RA. Estimation and variability of D90 as a function of seed detectability rates: Do all seeds need to be detected in order to compute useful Intraoperative dosimetry during prostate brachytherapy? Int. J. Radiat. Oncol. Biol. Phys 2004;60:S596–S597.

[17]. Su Y, Davis BJ, Herman MG, Manduca A, Robb RA. Examination of dosimetry accuracy as a function of seed detection rate in permanent prostate brachytherapy. Med. Phys 2005;32:3049–3056. [PubMed: 16266119]

[18]. Greenleaf JF, Fatemi M, Insana MF. Selected methods for imaging elastic properties of biological tissues. Ann. Rev. Biomed. Eng 2003;5:57–78. [PubMed: 12704084]

[19]. Fatemi M, Manduca A, Greenleaf JF. Imaging elastic properties of biological tissues by low-frequency harmonic vibration. Proc. IEEE 2003;91:1503–1519.

[20]. Gao L, Parker KJ, Lerner RM, Levinson SF. Imaging of the elastic properties of tissue - A review. Ultrasound Med. Biol 1996;22:959–977. [PubMed: 9004420]

[21]. Negron LA, Viola F, Black EP, Toth CA, Walker WF. Development and characterization of a vitreous mimicking material for radiation force imaging. IEEE Trans. Ultrason. Ferroelectr. Freq. Control 2002;49:1543–1551. [PubMed: 12484477]

[22]. Nightingale K, Soo MS, Nightingale R, Trahey G. Acoustic radiation force impulse imaging: in vivo demonstration of clinical feasibility. Ultrasound Med. Biol 2002;28:227–235. [PubMed: 11937286]

[23]. Xie H, Kim K, Aglyamov SR, Emelianov SY, Chen X, O'Donnell M, Weitzel WF, Wrobleski SK, Myers DD, Wakefield TW, Rubin JM. Staging deep venous thrombosis using ultrasound elasticity imaging: Animal model. Ultrasound Med. Biol 2004;30:1385–1396. [PubMed: 15582239]

[24]. Alizad A, Whaley DH, Greenleaf JF, Fatemi M. Potential applications of vibro-acoustography in breast imaging. Technol. Cancer Res. Treat 2005;4:151–157. [PubMed: 15773784]

[25]. Fatemi M, Greenleaf JF. Ultrasound-stimulated vibro-acoustic spectrography. Science 1998;280:82–85. [PubMed: 9525861]

[26]. Mitri FG, Davis BJ, Greenleaf JF, Fatemi M. Comparative study of vibro-acoustography versus pulse-echo ultrasound in imaging permanent prostate brachytherapy seeds. Ultrasonics Accepted. 2008(in press)

[27]. Mitri FG, Trompette P, Chapelon JY. Improving the use of vibro-acoustography for brachytherapy metal seed imaging: A feasibility study. IEEE Trans. Med. Imag 2004;23:1–6.

[28]. Ghiglia, DC.; Pritt, MD. Algorithms, and Software. John Wiley & Sons, Inc.; New York, NY: 1998. Two-Dimensional Phase Unwrapping--Theory.

[29]. Suh JH, Gardner JM, Kee KH, Shen S, Ayala AG, Ro JY. Calcifications in prostate and ejaculatory system: a study on 298 consecutive whole mount sections of prostate from radical prostatectomy or cystoprostatectomy specimens. Ann. Diag. Path 2008;12:165–170.

[30]. Gibbs NM, Price JL, Ainsworth RW, Korpal K. A radiological and histological study of prostatic calcification associated with primary carcinoma; a comparison with mammary microcalcification. Clin. Oncol 1975;1:305–313.

[31]. Urban MW, Kinnick RR, Greenleaf JF. Measuring the phase of vibration of spheres in a viscoelastic medium as an image contrast modality. J. Acoust. Soc. Am 2005;118:3465–3472. [PubMed: 16419793]

[32]. Silva GT, Greenleaf JF, Fatemi M. Linear arrays for vibro-acoustography: A numerical simulation study. Ultrasonic Imaging 2004;26:1–17. [PubMed: 15134390]

[33]. Davis BJ, Kinnick RR, Fatemi M, Lief EP, Robb RA, Greenleaf JF. Measurement of the ultrasound backscatter signal from three seed types as a function of incidence angle: Application to permanent prostate brachytherapy. Int. J. Radiat. Oncol. Biol. Phys 2003;57:1174–1182. [PubMed: 14575850]

[34]. Fatemi M, Wold LE, Alizad A, Greenleaf JF. Vibro-acoustic tissue mammography. IEEE Trans. Med. Imag 2002;21:1–8.

[35]. Alizad A, Fatemi M, Wold LE, Greenleaf JF. Performance of vibro-acoustography in detecting microcalcifications in excised human breast tissue: A study of 74 tissue samples. IEEE Trans. Med. Imag 2004;23:307–312.

[36]. Fatemi M, Greenleaf JF. Vibro-acoustography: An imaging modality based on ultrasound-stimulated acoustic emission. Proc. Natl. Acad. Sci. USA 1999;96:6603–6608. [PubMed: 10359758]

[37]. Patton CA, Harris GR, Phillips RA. Output Levels and Bioeffects Indexes from Diagnostic Ultrasound Exposure Data Reported to the FDA. IEEE Trans. Ultrason. Ferroelectr. Freq 1994;41:353–359.

[38]. French D, Morris J, Keyes M, Goksel O, Salcudean S. Computing intraoperative dosimetry for prostate brachytherapy using TRUS and fluoroscopy. Acad. Rad 2005;12:1262–1272.

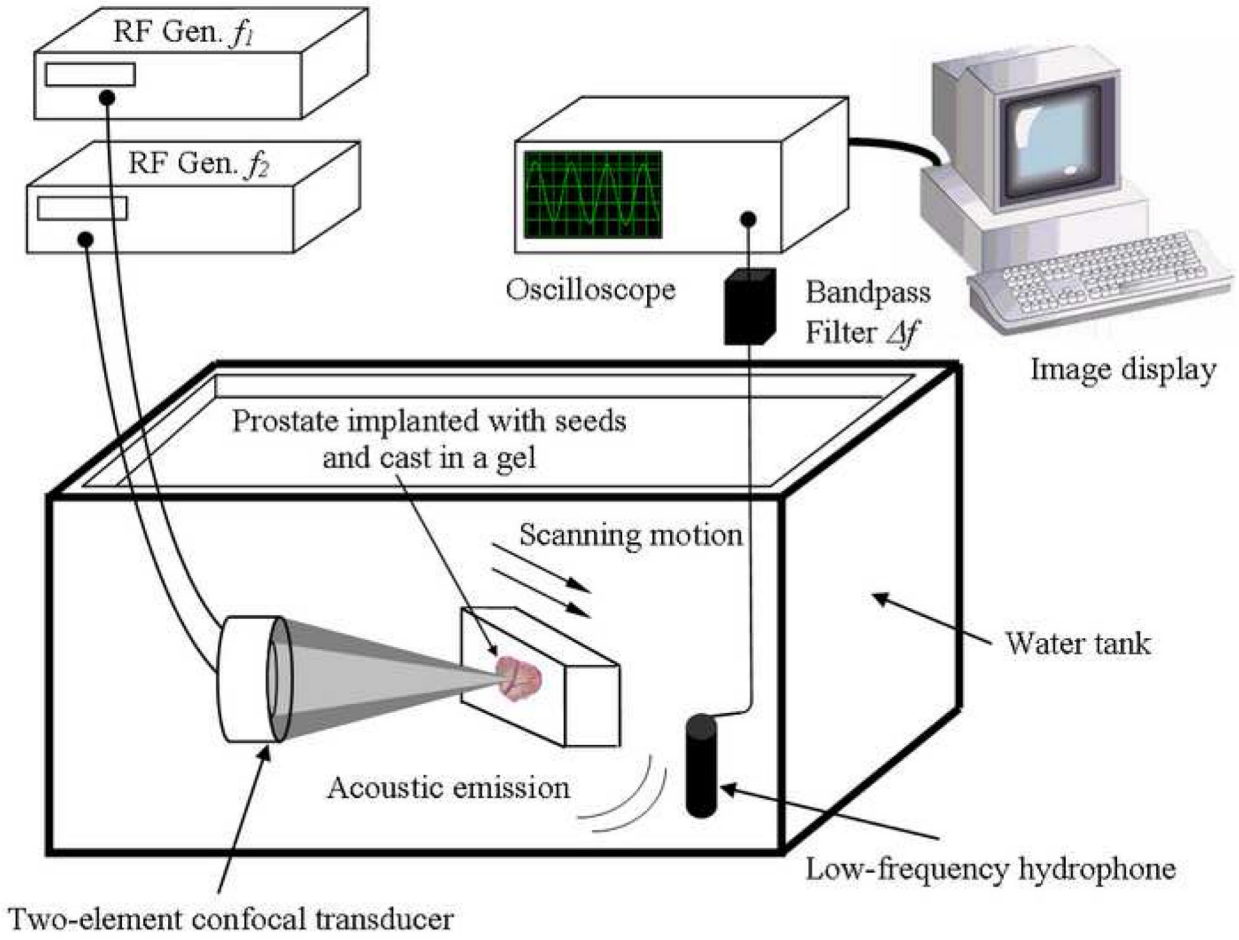

Figure 1.
Experimental VA system diagram. The excised prostate gland implanted with BT seeds is cast in a gel and placed within a water tank at the focus of the confocal ultrasound transducer and scanned at a desired depth inside the sample. The two ultrasound beams differ in frequency by Δf. The hydrophone receives the acoustic emission signal (at Δf) from the prostate. This signal is processed and mapped into an image. [Modified with permission from Ref. 27]

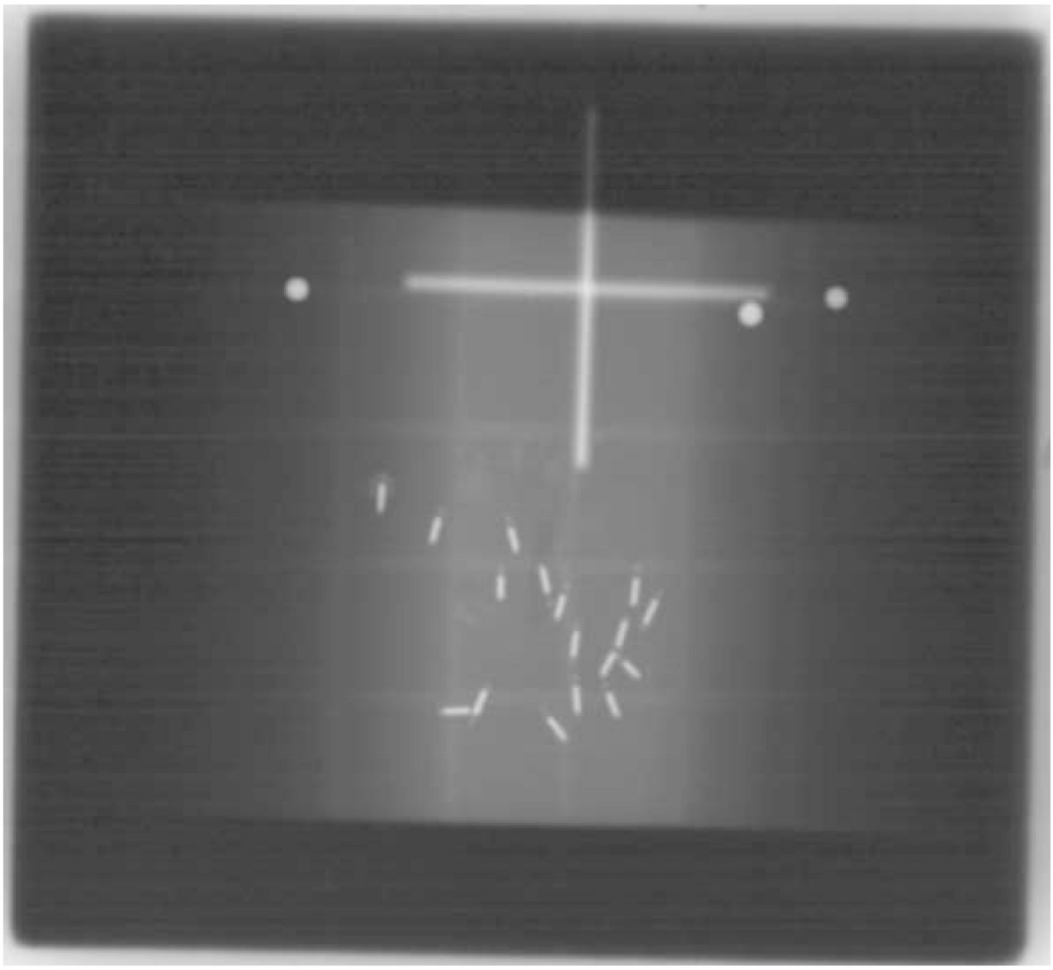

Figure 2.
X-ray of the cadaver prostate after prostatectomy. Seventeen seeds remained in the prostate after RRP. Intra-prostatic calcifications are faintly visible since the image was taken at 100 kVp. The three identification pins of a spherical end shape appear as bright spherical dots in the top of the image. These pins attached to the gel phantom at different locations have served as a reference for imaging.

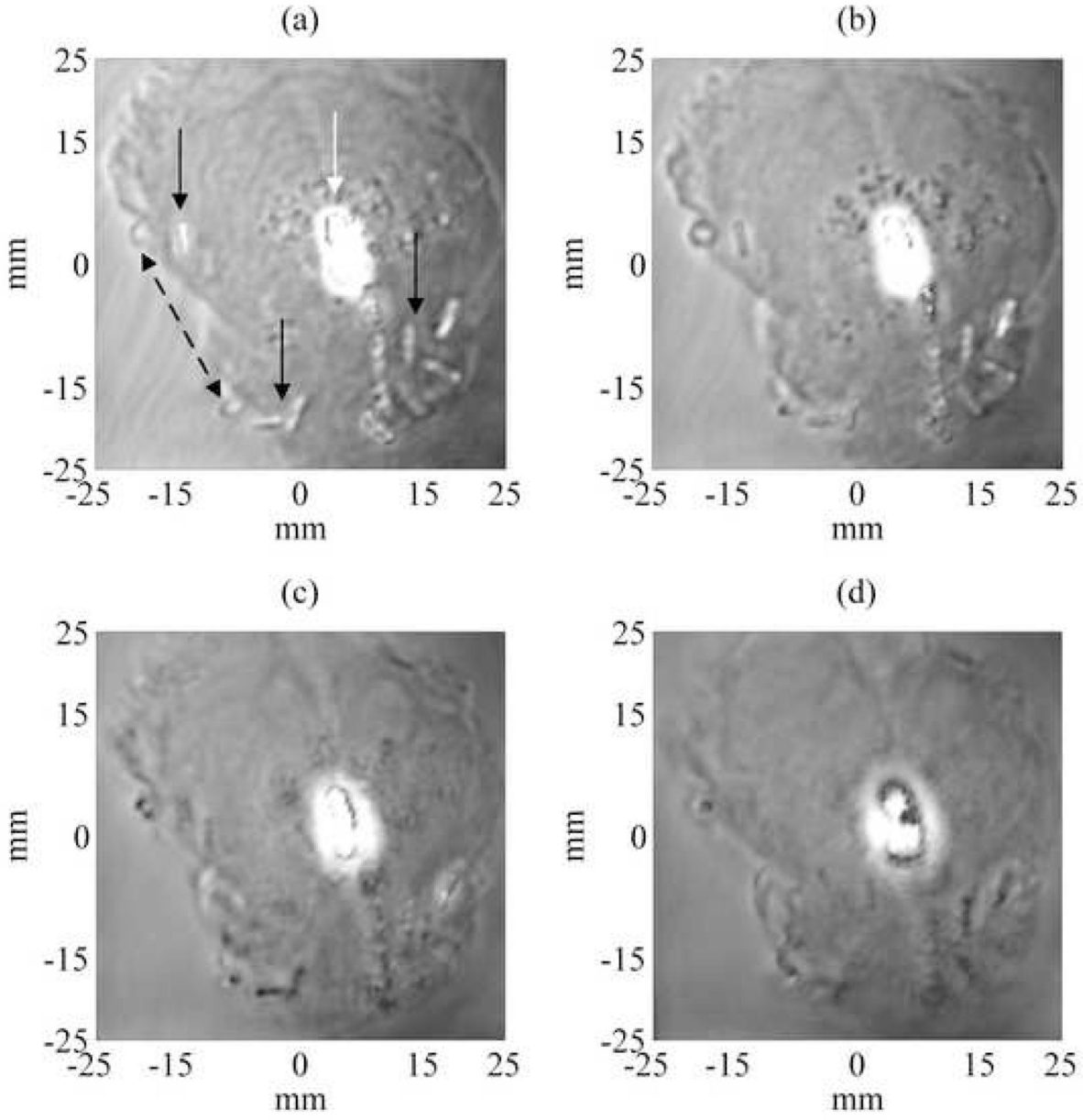

Figure 3.

Experimental magnitude VA images of the excised prostate showing seed location for 4 different depths at 1, 5, 10 and 15 mm (Figs. (a)-(d) respectively) deep from the surface of the prostate gland. The images covered an area of 50 mm by 50 mm, scanned at 0.25 mm/pixel incremental step. These VA images show some of the seeds (pointed by continued black arrows in (a)) at various angles and other seeds appeared more clearly at different depths. One notices also that the intra-prostatic calcifications (pointed by a white arrow in (a)) developed near the center of the prostate gland reflect ultrasound waves and thus obscure some of the seeds. The dotted black double-arrow points to gas bubbles that were developed at the interface prostatic tissue-gelatin after embedding the prostate in the gel phantom.

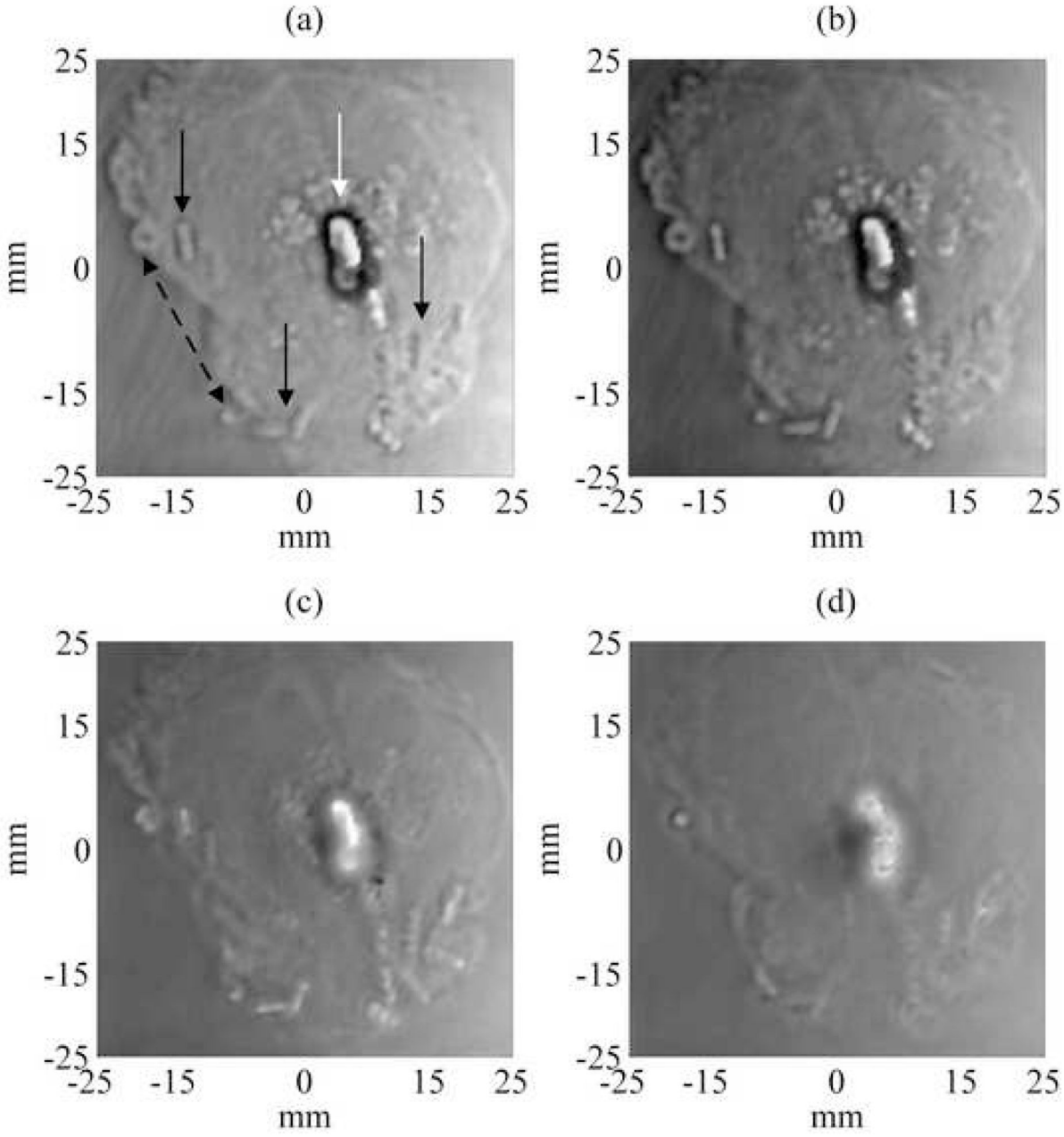

Figure 4.

Experimental unwrapped phase VA images of the excised prostate showing seed location for 4 different depths at 1, 5, 10 and 15 mm (Figs. (a)-(d) respectively) deep from the surface of the prostate gland. Displaying the unwrapped phase of the acoustic emission provides another source of image contrast for examining the prostate tissue and embedded objects. The unwrapped phase of the acoustic emission from prostate tissue is relatively constant. The unwrapped phase contrast of the calcification differs with the depth of the focal plane. The border of the calcification is well-defined and the brachytherapy seeds are well visualized at focal depths of 1-10 mm (i.e. Figs. 4-(a)-(c)).